Check for updates

Received: 4 September 2024 | Revised: 6 December 2024 | Accepted: 22 December 2024

DOI: 10.1002/cac2.12650

CANCER COMMUNICATIONS Open Access

LETTER TO THE JOURNAL

A strong internal promoter drives massive expression of YEATS-domain devoid *MLLT3* transcripts in HSC and most lethal AML

The AF9 (protein AF9) transcription factor, encoded by *MLLT3* (*mixed-lineage leukemia translocated to 3*) on chromosome 9, functions as a chromatin reader. Through its N-terminal YEATS (Yaf9, ENL, AF9, Taf14, and Sas5) protein domain, it interacts with acetylated [1] or crotonylated [2] histone H3, as well as with the PAF1 (RNA polymerase II-associated factor 1 homolog) and P-TEFb (positive transcription elongation factor b) components of the super elongation complex (SEC). AF9 also interacts through its poly-serine domain (Poly-Ser) with the TFIID (Transcription factor II D) subunit of the RNA polymerase II (RNApol II) complex. In addition, its C-terminal transactivation domain, AHD (nuclear anchorage protein1 homology domain), binds other SEC components, such as AFF1 and AFF4 (ALF transcription elongation factor 1 or 4), as well as transcription regulators CBX8 (chromobox 8), DOT1L (disruptor of telomeric silencing 1 like), and BCOR (B cell lymphoma 6 corepressor), as reviewed by Kabra & Bushweller [3] (Figure 1A). Thus, MLLT3 is an integral part of the SEC, which is essential for optimizing the catalytic activity of RNApol II transcription at specific genome loci.

Several studies have indicated that *MLLT3* is highly and specifically expressed in hematopoietic stem cells (HSCs), but it is rapidly and significantly downregulated during normal differentiation or immediately after HSCs are placed in *ex vivo* culture. In both scenarios, this shutdown parallels the rapid loss of stemness. Consistently, ectopic expression of *MLLT3* significantly prolongs self-renewal capacity of HSCs, suggesting that *MLLT3* is a crucial factor for HSC maintenance [4].

Based on standard quantification of RNA-sequencing reads mapping to the *MLLT3* locus, we first confirmed that, compared to the *MLLT1* paralogue used as an internal control, *MLLT3* expression was significantly higher in $CD34^+$ cells than in mature lymphocytes, granulocytes, or monocytes from healthy samples of the Leucegene dataset (Leucegene-NH, detailed in Supplementary Information) (Figure 1B, left panel). To refine this observation, made in $CD34^+$ cells containing a mixture of progenitors but only a few HSCs, we repeated the analysis in HSCs and various stages of progenitor cells sorted form healthy donors (IUCT-NH, detailed in Supplementary Information). The data clearly confirmed that *MLLT3* is highly expressed in HSCs but rapidly declines as differentiation proceeds (Figure 1B, right panel).

However, closer examination using a k-mer approach (described in Materials and Methods in Supplementary Information), which visualized RNA-sequencing read alignment along the 11 exons (E1-E11) of the reference *MLLT3* transcript, revealed an unexpected profile. Strikingly, the substantial *MLLT3* expression detected in HSCs was driven by a sharp and pronounced increase in reads starting precisely at the first nucleotide of exon E6 (Figure 1C). This unexpected profile was absent when examining *MLLT1* expression in the hematopoietic lineage (Supplementary Figure S1). These findings suggest the expression of one or more 5' end shortened *MLLT3*

Abbreviations: AF9, Protein AF9; AFF1/4, ALF Transcription Elongation Factor 1 or 4; AHD, ANC1 (nuclear anchorage protein 1) homology domain; AML, Acute myeloid leukemia; BCOR, BCL6 (B Cell Lymphoma 6) corepressor; CBX8, Chromobox 8; CD14, Monocyte differentiation antigen CD14; CD34, Hematopoietic progenitor cell antigen CD34; DOT1L, Disruptor of telomeric silencing 1 like (a histone lysine methyltransferase); ELN2017, European LeukemiaNet 2017; GATA2, GATA Binding Protein 2; HSC, Hematopoietic stem cell; IUCT, Institut Universitaire du cancer de Toulouse; KMT2A, Lysine (K) methyl-transferase 2A; MECOM, MDS1 (Myelodysplasia syndrome 1) and EVI1 (Ecotropic virus integration site 1) complex locus; MLLT1/3, Mixed-lineage leukemia translocated to, 1 or 3; PAF1, RNA polymerase II-associated factor 1 homolog; Poly-Ser, Poly-serine; P-TEFb, Positive transcription elongation factor b; RNApol II, RNA polymerase II; RUNX1, Runt-related transcription factor 1; SEC, Super elongation complex; TFIID, Transcription factor II D; TP53, Tumor protein p53; YEATS, Yaf9, ENL, AF9, Taf14, and Sas5 (the five first proteins shown as containing such domain).

[†]Chloé Bessière, Ahmed Zamani, and Romain Pfeifer contributed equally.

This is an open access article under the terms of the Creative Commons Attribution-NonCommercial-NoDerivs License, which permits use and distribution in any medium, provided the original work is properly cited, the use is non-commercial and no modifications or adaptations are made.
© 2025 The Author(s). *Cancer Communications* published by John Wiley & Sons Australia, Ltd. on behalf of Sun Yat-sen University Cancer Center.

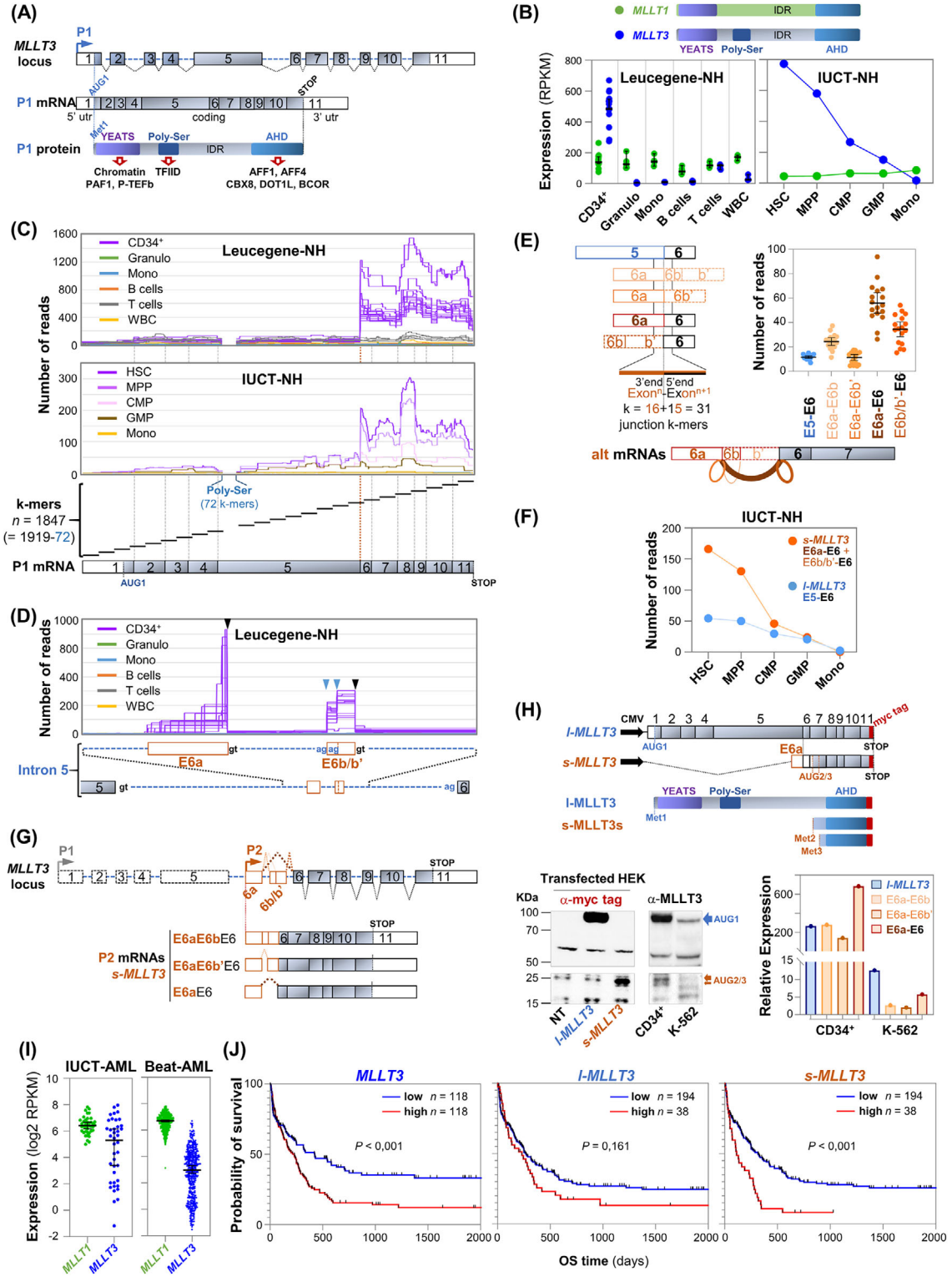

FIGURE 1 A strong internal promoter drives massive expression of YEATS-domain devoid *MLLT3* transcripts in HSC and most lethal AML. (A) Next to its P1 promoter, the *MLLT3* locus is transcribed into a P1 mRNA encompassing 11 exons (E1 to E11) and coding for a P1 protein starting at AUG1 (encoding Met1), which contains three characterized functional domains (YEATS, Poly-Ser, and AHD) that interact with other transcriptional regulators (see text for details). (B) To establish the expression profile of *MLLT3* in the hematopoietic lineage versus that of its paralog *MLLT1* (top), which serves as an internal control, quantification of the global expression of their respective mRNAs was performed using standard procedures in two RNA-Seq cohorts containing healthy donor samples (bottom). The Leucegene-NH dataset included sorted CD34$^+$CD45RA$^-$ cord blood cells ($n = 17$), granulocytes ($n = 5$), monocytes ($n = 5$), B cells ($n = 5$), T cells ($n = 5$), and unsorted white blood cells (WBC, $n = 3$) from individual donors (left). The local IUCT-NH dataset (see Supplementary Information for details) contained hematopoietic differentiation intermediates sorted from a pool ($n = 30$) of healthy donors (right). Bars: median with 95%

25233548, 0, Downloaded from https://onlinelibrary.wiley.com/doi/10.1002/cac2.12650, Wiley Online Library on [06/01/2025]. See the Terms and Conditions (https://onlinelibrary.wiley.com/terms-and-conditions) on Wiley Online Library for rules of use; OA articles are governed by the applicable Creative Commons License

transcripts arising from a hematologic lineage-specific internal promoter located in *MLLT3* intron 5.

A new set of specific and successive k-mers covering the entire *MLLT3* intron 5 revealed the presence of two novel segments retained in poly(A)$^+$ RNAs. Apart from the 5' end of the first segment, which lacked a clearly defined starting point consistent with a probable transcription start site, consensus donor and acceptor splice sites flanked these

confidence interval (CI). The data showed a high level of *MLLT3* expression in HSCs that rapidly declined as differentiation proceeded, while *MLLT1* expression remained relatively constant. (C) To observe how RNA-Seq reads distribute along the 11 exons (E1-E11) of the *MLLT3* transcript (X-axis, P1 mRNA), a k-mer quantification (Y-axis, normalized number of reads) was performed on the two Leucegene-NH (top) and IUCT-NH (bottom) datasets described above. The 1949 nucleotides composing the reference *MLLT3* transcript (NM_004529.4, from its 5'end to the stop codon) yielded 1919 consecutive k-mers where k = 31 (31-mers). To avoid bias in data interpretation, 72 k-mers covering the Poly-Ser-coding repeat sequence were excluded from the graphs (i.e., 1919-72 = 1847 k-mers). An unexpected profile was obtained in HSCs and progenitor cells, with a sharp and strong increase in the number of reads occurring at the very first nucleotide of E6, which became progressively less marked as differentiation proceeded. (D) To detect potentially novel *MLLT3* sequence segments that could be retained in poly(A)$^+$ RNAs, a k-mer quantification of RNA-Seq-reads (Y-axis, normalized number of reads) mapping to reference *MLLT3* intron 5 (NM_004529.4, X-axis) was performed in the Leucegene-NH dataset. This revealed the existence of two additional segments embedded in intron 5, upstream from exon 6 and flanked by donor (gt, black arrowhead) and acceptor (ag, blue arrowhead) splicing sites. These two novel exons were named E6a and E6b/b'. (E) To verify whether the novel exons E6a and/or E6b/b' could compete with exon 5 for splicing to exon E6, we designed new k-mers covering the possible alternative exon-exon junctions as follows: the last 16 nucleotides (3'end) of exon n joined to the first 15 nucleotides (5'end) of exon n+1 (i.e. k = 16+15 = 31) (left, as described in Supplementary information). Then, RNA-Seq reads covering these putative exon-exon junctions were quantified using the k-mer technique in individual CD34$^+$ samples (n = 17) from the Leucegene-NH dataset (right). Bars: mean with 95% CI. The thickness of arcs below is proportional to the number of reads covering the new alternative exon-exon junctions (bottom). This quantification revealed that all possible exon-exon assortments existed, including the three alternative transcripts E6a-E6b-E6, E6a-E6b'-E6 and E6a-E6 (alt mRNAs), with the E6a-E6 variant being the most abundant in CD34$^+$ cells. (F) After naming the shorter alternative transcripts driven by the internal promoter as *s-MLLT3* (compared to the full transcript named *l-MLLT3*), we returned to the IUCT-NH samples (those used in Figure 1B, bottom right, and showing overall *MLLT3* expression) and measured how their relative expression evolved from HSCs through differentiation intermediates to monocytes. Quantification using isoform-specific k-mers (performed as described above) confirmed that the shorter *s-MLLT3* transcripts were expressed at much higher levels in HSCs than the *l-MLLT3* transcript, and that their expression decreased as differentiation proceeded. (G) Schematic representation of the *MLLT3* locus highlighting the P2 internal promoter-driven *s-MLLT3* transcripts (P2 mRNAs). (H) To examine the coding potential of s-MLLT3 transcripts, the HEK test cell line was transfected with CMV-promoted pcDNA3 vectors, resulting in the expression of myc-tagged *s-MLLT3* or *l-MLLT3* transcripts (as control) at the 3'-end (top). Visualization of the corresponding proteins (arrows) by western-blotting, as previously described [9], using anti-myc tag antibodies (bottom left), revealed that, compared with cells transfected with the *l-MLLT3* vector (where a full-size protein was detected), two much smaller bands appeared in cells transfected with the E6a-E6 *s-MLLT3* vector. Their smaller sizes matched with the presence of two AUG codons in exon 7 (AUG2/3, as shown in the top scheme). Endogenous expression of these two shorter proteins was confirmed by western blotting performed on extracts of CD34$^+$ (and of K-562 leukemia cells as a low-expressing control) using an MLLT3-specific antibody (bottom middle). As shown by RT-qPCR quantification, compared to CD34$^+$ cells and to full length *l-MLLT3*, expression of the three E6a-E6b, E6a-E6b', and E6a-E6 s-*MLLT3* shorter forms was very low in K-562 cells (bottom right). (I) To measure expression from the *MLLT1* and *MLLT3* loci in AML, quantifications were performed using standard bioinformatics procedures in two RNA-Seq datasets: IUCT-AML and Beal-AML. Although lower than that of *MLLT1*, *MLLT3* expression appeared much more variable. (J) Given that different transcript isoforms encoding different MLLT3 proteins were not equally expressed in all AML samples, the overall survival (OS) time (days) was monitored by Kaplan-Meier curves on Beat-AML patients as a function of either global *MLLT3* (left), *l-MLLT3* (middle), or *s-MLLT3* (right) expression. To avoid potential bias in data interpretation, as previously described [10], samples that were not collected at diagnosis but later after the first line of therapy, those presenting at diagnosis with no AML but with an MDS or MPN, and the samples from patients who could benefit from a transplant, were removed. The curves were finally calculated with this homogeneous set of n = 236 patients, from the date of diagnosis until death or last received news. Surviving patients were censored at the date of the last follow-up. Log-rank test was used for statistics. Global *MLLT3* expression was quantified using standard pipelines, while *l-MLLT3* or *s-MLLT3* were quantified using isoform specific k-mers as described in Figure 1E and 1F. For global *MLLT3* expression, the cohort was divided into two categories based on median expression. For *l-MLLT3* or *s-MLLT3*, the cohort was divided into a "high" category comprising the ~20% of samples with the highest level of *l-MLLT3* or *s-MLLT3* (n = 38/236 in each case) and a "low" category comprising the ~80% of samples with the lowest level of *l-MLLT3* or *s-MLLT3* (n = 194/236 in each case). These analyses indicated that overall *MLLT3* expression is of poor prognosis (left), and that the ~20% of patients with the highest level of *s-MLLT3* had a much worse prognosis than the ~20% of patients with the highest level of *l-MLLT3* (compare right and middle panels). Abbreviations: utr: Untranslated region; IDR: Intrinsically disordered region; NH: Normal hematopoiesis; HSC: Hematopoietic stem cell; MPP: Multipotent progenitor, CMP: Common myeloid progenitor; GMP: Granulo-monocytic progenitor; Mono: Monocyte. WBC: White blood cells; IUCT: Institut Universitaire du Cancer; CMV: Cytomegalovirus; HEK: Human embryonic kidney; NT: Not transfected; OS: Overall survival; MDS: Myelodysplastic syndrome; MPN: Myeloproliferative neoplasm; RT: Reverse transcription; qPCR: quantitative Polymerase chain reaction.

25233548, 0, Downloaded from https://onlinelibrary.wiley.com/doi/10.1002/cac2.12650, Wiley Online Library on [06/01/2025]. See the Terms and Conditions (https://onlinelibrary.wiley.com/terms-and-conditions) on Wiley Online Library for rules of use; OA articles are governed by the applicable Creative Commons License

two segments. These unexpected exons were designated as exon E6a and exon E6b/b' (Figure 1D). Additional k-mer analyses confirmed that these exons were spliced to exon E6, resulting in three possible splice variants: E6a-E6b-E6, E6a-E6b'-E6, and E6a-E6, with the E6a-E6 variant being the most predominant (Figure 1E and Supplementary Figure S2). This assortment of novel $CD34^+$-specific alternative exons was further validated using standard Sanger sequencing following RT-PCR amplification with specific primers (Supplementary Figure S3).

Next, exploration of public CHIP-Seq (chromatin immunoprecipitation followed by sequencing) and CAGE (mRNA 5' cap analysis of gene expression) datasets revealed the existence of an alternative P2 promoter in addition to the canonical P1 promoter. Associated with an active promoter H3K4me3 mark and a CAGE peak, this P2 promoter, found exclusively in immature $CD34^+$ cells but absent in $CD14^+$ monocytes, was predicted to drive the expression of transcripts beginning with exon E6a (Supplementary Figure S4). Transcript-specific k-mer quantifications confirmed that the exceptionally high overall level of *MLLT3* observed in HSCs was primarily due to these shorter transcripts starting with exon E6a. We have collectively named these shorter transcripts *s-MLLT3*, in contrast to the reference full-length *MLLT3* transcript, referred to as *l-MLLT3* (Figure 1F).

These findings revealed the existence of an HSC-specific internal promoter (P2) that drives the expression of shorter *MLLT3* transcripts (*s-MLLT3* mRNAs, Figure 1G). To evaluate the translational potential of these *s-MLLT3* transcripts, we cloned a C-terminal myc-tagged version of the predominant E6a-E6 variant into an expression vector (Figure 1H, top), and assessed its protein expression capacity in the HEK (human embryonic kidney) cell line by western blotting. Compared with a similar vector encoding *l-MLLT3*, the E6a-E6 *s-MLLT3* transcript produced shorter s-MLLT3 proteins, (Figure 1H, bottom left). A western blotting analysis of endogenous proteins confirmed the existence of these shorter forms in $CD34^+$ cells but not in the K-562 leukemic cell line, which served as a low-expressing control (Figure 1H, bottom middle). Isoform-specific RT-qPCR quantification further corroborated that, compared to $CD34^+$ cells and full-length *l-MLLT3*, expression of the three shorter forms (E6a-E6b, E6a-E6b', and E6a-E6) was very low in K-562 cells (Figure 1H, bottom right). These western blot results identified at least two distinct s-MLLT3 proteins, likely arising from alternative translation initiation codons (AUG2 and AUG3) located in exon 7, producing proteins that retain the C-terminal AHD transactivation domain but lack the YEATS and Poly-Ser domains (Supplementary Figure S5).

Interestingly, the shorter *MLLT3* alternative transcripts initiate within intron 5, which is also a frequent site of chromosomal translocation in acute myeloid leukemia (AML). Specifically, *MLLT3* intron 5 is the primary site of the t(9;11) chromosomal translocation, leading to fusion with *KMT2A* (lysine (K) methyl transferase 2A) [5]. KMT2A is a chromatin writer that deposits epigenetic marks indicating active transcription at specific loci, particularly the *HOX* genes required for hematopoiesis [6]. The resulting *KMT2A-MLLT3* fusion transcript encodes a chimeric protein composing the N-terminal third of KMT2A fused to the C-terminal portion of MLLT3, which lacks the YEATS domain but retains the AHD transactivation domain (Supplementary Figure S6). To investigate global *MLLT3* expression in AML, we analyzed two RNA-Seq datasets: IUCT-AML [7] and Beat-AML [8] (detailed in Supplementary Information). Compared with *MLLT1*, the expression range of *MLLT3* was broader, showing a > 120-fold amplitude across samples (Figure 1I). Isoform-specific k-mers targeting alternative (E6a-E6 + E6b/b'-E6 for *s-MLLT3*) and canonical (E5-E6 for *l-MLLT3*) exon-exon junctions revealed no correlation between *s-MLLT3* and *l-MLLT3* expressions. Approximately 20% of samples exhibited high *s-MLLT3* levels, whereas in other samples, *s-MLLT3* was undetectable despite *l-MLLT3* expression (Supplementary Figure S7). This finding suggests differential regulation of the two promoters and/or the resulting transcripts in AML.

We next investigated whether the ~20% of AML samples with high *s-MLLT3* expression represented a distinct clinical entity. Samples which were either $MECOM^+$ (myelodysplasia syndrome 1 and EVI1 complex locus) or *GATA2-MECOM* (Supplementary Figure S8), and those with mutant *RUNX1* (runt-related transcription factor 1) and/or *TP53* (tumor protein p53) showed higher levels of *l-MLLT3*, with even greater levels of *s-MLLT3* (Supplementary Figure S9, left and middle). No correlation with the *KMT2A-MLLT3* translocation was observed. Conversely, *NPM1* (nucleophosmin 1)-mutated samples exhibited very low levels of both transcripts (Supplementary Figure S9, left and middle). Notably, elevated *s-MLLT3* or *l-MLLT3* levels were associated with an adverse ELN2017 (European LeukemiaNet 2017) score (Supplementary Figure S9, right). Median expression-based group separation revealed that patients with the highest overall *MLLT3* expression had worse survival outcomes (Figure 1J, left). However, given the lack of correlation between *s-MLLT3* and *l-MLLT3* expression in AML samples, we assessed their independent impacts on survival. Isoform-specific k-mers showed that *s-MLLT3* (but not *l-MLLT3*) expression significantly influenced poor patient survival (Figure 1J, middle and right panels).

25233548, 0, Downloaded from https://onlinelibrary.wiley.com/doi/10.1002/cac2.12650, Wiley Online Library on [06/01/2025]. See the Terms and Conditions (https://onlinelibrary.wiley.com/terms-and-conditions) on Wiley Online Library for rules of use; OA articles are governed by the applicable Creative Commons License

In conclusion, these findings demonstrate the existence of an internal promoter within the *MLLT3* locus, driving expression of 5'-end-shortened transcripts encoding an AF9 protein lacking the YEAST chromatin reader domain. These alternative transcripts are highly expressed in HSCs and in ∼20% of AML patients with the worst survival outcomes. These results suggest that the role of the *MLLT3* locus in HSCs and in AML should be re-evaluated, considering the expression of this YEATS-domain-devoid AF9 transcription factor.

AUTHOR CONTRIBUTIONS

Stéphane Pyronnet wrote the manuscript. Chloé Bessière, Ahmed Zamani, Sandra Dailhau, Christian Récher, Marina Bousquet, and Stéphane Pyronnet contributed to the study design, conception, and data analysis. Ahmed Zamani, Romain Pfeifer, and Marina Bousquet designed and performed biological experiments. Chloé Bessière, Sandra Dailhau, Camille Marchet, Benoit Guibert, Anthony Boureux, Raïssa Silva Da Silva, Nicolas Gilbert, and Thérèse Commes developed the k-mer-based bioinformatics tools. Fabienne Meggetto, Christian Touriol, and Marina Bousquet provided comments on and contributed to editing the manuscript.

ACKNOWLEDGEMENTS

Some of the results presented in this publication are based on data generated by the Leucegene group, primarily based at IRIC in Montreal, Canada, and supported by Genome Canada and Genome Québec. This data was made possible through human AML specimens provided by the BCLQ in Montreal, Canada.

CONFLICT OF INTEREST STATEMENT

Christian Récher declares a consulting or advisory role with Abbvie, Amgen, Astellas, BMS, Boehringer, Jazz Pharmaceuticals, and Servier, and has received research funding from Abbvie, Amgen, Astellas, BMS, Iqvia, and Jazz Pharmaceuticals. All other authors declare no conflict of interest.

FUNDING INFORMATION

This work was funded by INSERM, Institut Universitaire du Cancer-Toulouse (IUCT), Labex Toucan, Fondation Leucémie Espoir, Ligue Régionale Contre le Cancer, Fondation ARC, Association Laurette Fugain, Agence Nationale de la Recherche (ANR-18-CE45-0020 Transipedia) and (ANR-22-CE45-0007 full-RNA). Chloé Bessière was supported by Fondation de France, Ahmed Zamani and Raïssa Silva Da Silva by Ligue Nationale Contre le Cancer, Romain Pfeifer by Ministère de l'Enseignement Supérieur et de la Recherche and Fondation ARC, Sandra Dailhau by Ministère de la Santé and Institut National du Cancer (INCA, PRT-K-2022-184CircOma).

ETHICS APPROVAL AND CONSENT TO PARTICIPATE

In accordance with French law, each anonymous volunteer donor or patient was informed, and the HIMIP collection has been declared to the Ministère de l'Enseignement Supérieur et de la Recherche (DC 2008-307). A transfer agreement was obtained (AC 2008-129) after approval by the local ethical committee, Comité de Protection des Personnes Sud-Ouest et Outremer II, and the local Research Ethics Committee of the Etablissement Français du Sang (Toulouse, France, agreement #21PLER2021-007). Clinical and biological annotations have also been declared to the Comité National Informatique et Libertés (CNIL). This study was conducted in accordance with the Declaration of Helsinki.

DATA AVAILABILITY STATEMENT

The raw and processed RNA-sequencing data generated in this study have been deposited at the National Center for Biotechnology Information Gene Expression Omnibus (repository number GSE62852).

Chloé Bessière[1,2,†]
Ahmed Zamani[1,†]
Romain Pfeifer[1,†]
Sandra Dailhau[1]
Camille Marchet[3]
Benoit Guibert[2]
Anthony Boureux[2]
Raïssa Silva Da Silva[2]
Nicolas Gilbert[2]
Thérèse Commes[2]
Fabienne Meggetto[1]
Christian Touriol[1]
Christian Récher[4]
Marina Bousquet[1]
Stéphane Pyronnet[1]

[1]*Cancer Research Center of Toulouse, INSERM UMR-1037, CNRS UMR-5071, Toulouse University, Toulouse, France*
[2]*Institute for Regenerative Medicine and Biotherapy, INSERM UMR-1183, Saint-Éloi Hospital, Montpellier University, Montpellier, France*
[3]*CRIStAL-Research center in Computer Science, Signal and Automatic Control of Lille, CNRS UMR-9189, Lille University, Villeneuve d'Ascq, France*
[4]*Hematology Department, University Hospital Center, IUCT-University Cancer Institute, Toulouse, France*

25233548, 0, Downloaded from https://onlinelibrary.wiley.com/doi/10.1002/cac2.12650, Wiley Online Library on [06/01/2025]. See the Terms and Conditions (https://onlinelibrary.wiley.com/terms-and-conditions) on Wiley Online Library for rules of use; OA articles are governed by the applicable Creative Commons License

Correspondence
Dr Stéphane Pyronnet and Dr Marina Bousquet, Cancer Research Center of Toulouse, 2 Hubert Curien Avenue, 31037 Toulouse, France.
Email: stephane.pyronnet@inserm.fr and marina.bousquet@inserm.fr

ORCID

Stéphane Pyronnet https://orcid.org/0000-0002-9562-5112

REFERENCES

1. Li Y, Wen H, Xi Y, Tanaka K, Wang H, Peng D, et al. AF9 YEATS domain links histone acetylation to DOT1L-mediated H3K79 methylation. Cell. 2014;159:558–571.
2. Li Y, Sabari BR, Panchenko T, Wen H, Zhao D, Guan H, et al. Molecular coupling of histone crotonylation and active transcription by AF9 YEATS domain. Mol Cell. 2016;62:181-193.
3. Kabra A, Bushweller J. The intrinsically disordered proteins MLLT3 (AF9) and MLLT1 (ENL) – multimodal transcriptional switches with roles in normal hematopoiesis, MLL fusion leukemia, and kidney cancer. J Mol Biol. 2022;434:167117.
4. Calvanese V, Nguyen AT, Bolan TJ, Vavilina A, Su T, Lee LK, et al. MLLT3 governs human haematopoietic stem-cell self-renewal and engraftment. Nature. 2019;576:281–286.
5. Meyer C, Larghero P, Almeida Lopes B, Burmeister T, Gröger D, et al. The KMT2A recombinome of acute leukemias in 2023. Leukemia. 2023;37(5):988–1005.
6. Milne TA, Briggs SD, Brock HW, Martin ME, Gibbs D, Allis CD, et al. MLL targets SET domain methyltransferase activity to Hox gene promoters. Mol Cell. 2002;10:1107–1117.
7. De Clara E, Gourvest M, Ma H, Vergez F, Tosolini M, Dejean S, et al. Long non-coding RNA expression profile in cytogenetically normal acute myeloid leukemia identifies a distinct signature and a new biomarker in NPM1-mutated patients. Haematologica. 2017;102:1718–1726.
8. Tyner JW, Tognon CE, Bottomly D, Wilmot B, Kurtz SE, Savage SL, et al. Functional genomic landscape of acute myeloid leukaemia. Nature. 2018;562:526–531.
9. Alard A, Marboeuf C, Fabre B, Jean C, Martineau Y, Lopez F, et al. Differential regulation of the three eukaryotic mRNA translation Initiation factor (eIF) 4Gs by the proteasome. Front Genet. 2019;10:254.
10. Corre E, Soum C, Pfeifer R, Bessière C, Dailhau S, Marbœuf C, et al. Differential prognostic values of the three AKT isoforms in acute myeloid leukemia. Sci Rep. 2024;14:7070.

SUPPORTING INFORMATION

Additional supporting information can be found online in the Supporting Information section at the end of this article.

25233548, 0, Downloaded from https://onlinelibrary.wiley.com/doi/10.1002/cac2.12650, Wiley Online Library on [06/01/2025]. See the Terms and Conditions (https://onlinelibrary.wiley.com/terms-and-conditions) on Wiley Online Library for rules of use; OA articles are governed by the applicable Creative Commons License